SUPPORTING INFORMATION

TiO_2 mesoporous thin films architecture as a tool to control Au nanoparticles growth and sensing capabilities

Paula Y. Steinberg[1,§], M. Mercedes Zalduendo[1,§], Gustavo Giménez[2], Galo J. A. A. Soler Illia[3], Paula C. Angelomé[1,*]

[1] Gerencia Química, Centro Atómico Constituyentes, Comisión Nacional de Energía Atómica, CONICET, Av. Gral. Paz 1499, B1650KNA San Martín, Buenos Aires, Argentina.
[2] Centro de Micro y Nanoelectrónica del Bicentenario, INTI-CMNB, Instituto Nacional de Tecnología Industrial, San Martín, Buenos Aires, Argentina
[3] Instituto de Nanosistemas, UNSAM, CONICET, 25 de mayo 1021, 1650 San Martín, Buenos Aires, Argentina.

[§] These authors contributed equally to this work
[*] Corresponding author email: angelome@cnea.gov.ar

1. Mesoporous TiO_2 thin films (MTTFs) characterization

Ellipsometry and Environmental Ellipsometric Porosimetry

Ellipsometry measurements were carried out in an ellipsometer SOPRA GES5A. All samples were washed with ethanol and dried before measure. A micro-spot configuration was used to study a sample area of 1 mm^2. The refractive indexes of each film were obtained from data adjustment using Winelli II software.
The same equipment was used to determine pore and necks size distribution, by means of Environmental Ellipsometric Porosimetry.[1] The changes of ellipsometric parameters Ψ and Δ at variable vapor pressure of water at room temperature were measured. Data were fitted using a Forouhi-Bloomer dispersion law.[2] Pore size distributions were obtained from the adsorption-desorption isotherms using a model based on Kelvin equation.[1] Water contact angles, necessary for such modelling, were determined using a Ramé-Hart 190 CA equipment.

XRR data analysis and results

Film thickness was determined from the Kiessig fringes in the reflectogram. Film porosity was estimated by measuring the shift in the critical angle when the relative humidity (RH) was changed from <5% (i.e. the pores are full of air) to >90% (i.e. the pores are filled with water). Au loading fractions were calculated measuring the shift in the critical angle at a low humidity (<5%) before and after Au NPs synthesis inside the mesopores. For these purposes, the measurements were made with the films placed inside a controlled humidity chamber.

Kiessig oscillations in the higher angular region ($\theta > 3\theta_c$) allow defining the thickness (t) of the sample according to equation 1.

$$t = \frac{\lambda}{2\Delta\ (sin\theta)} \tag{1}$$

where λ is the wavelength of the monochromatic X-rays used (1.54 Å) and $\Delta\ (sin\theta)$ is the period of these oscillations.
The reflectivity critical angle θ_c (the angle at which the reflected intensity is half the total external reflection) allows determining the electronic density (ρ_e) of the film by using equation 2.

$$\rho_e = \frac{\pi}{\lambda^2 r_e}\theta_c^2 \tag{2}$$

where r_e is the classical radius of the electron (2.813×10^{-6} nm). Taking into account equation (2), the films' porosity can be estimated from XRR data by measuring the change in the critical angle (and thus, in the thin film density) when the relative humidity (RH) changes from <5% (i.e. the pores are full of air) to >90% (i.e. the pores are filled with water). For that purpose, XRR measurements were made with the films placed inside a controlled humidity chamber. Considering that the increase in film density is only due to the presence of water, the water volume fraction ($F_v(H_2O)$) within the film was determined from the measured electronic densities using equation 3.In this case, the $F_v(H_2O)$ calculated is equivalent to the porosity (P) of the material.

$$P = F_v(H_2O) = \frac{\rho_e(film\ +\ H_2O)\ -\ \rho_e(\ film)}{\rho_e(H_2O)} \tag{3}$$

Where $\rho_e(film + H_2O)$ is the electronic density of water-filled film (measured at RH>90%), $\rho_e(film)$ is the electronic density of the film (measured at RH<5%) and the $\rho_e(H_2O)$ is the water electronic density. Same approach was used to determine the Au filling fraction ($F(Au)$) using equation 4. The $F(Au)$ represents the fraction of the porosity that has been occupied with Au.

$$F_v(Au) = \frac{\rho_e(film\ +\ Au)\ -\ \rho_e(\ film)}{\rho_e(Au)};\quad F(Au) = \frac{F_v(Au)}{P} \tag{4}$$

where $F_v(Au)$ is the Au volume fraction, $\rho_e(film + Au)$ is the electronic density of Au loaded film (measured at RH < 5%), and $\rho_e(Au)$ is the gold electronic density.

Table S1. Films critical angle (θc), porosity (P) and thickness obtained by XRR measurements. Film´s average refractive index obtained by ellipsometry. Samples were obtained by dip-coating.

System	θc (°)	P (%)	Thickness (nm)	Refractive index
TB	0.19 ± 0.01	48 ± 2	150 ± 5	1.65
TF	0.19 ± 0.01	50 ± 2	165 ± 5	1.60
TP	0.16 ± 0.01	62 ± 2	180 ± 5	1.47

2. Synthesis of Au NPs inside MTTFs

Table S2. Plasmonic band maximum and full width at half maximum (FWHM) for *AuZRS@TX* samples, obtained from UV-vis absorption spectra.

	Z = 5		**Z = 10**		**Z = 15**		**Z = 20**	
	λ_{max}/nm	**FWHM/nm**	**λ_{max}/nm**	**FWHM/nm**	**λ_{max}/nm**	**FWHM/nm**	**λ_{max}/nm**	**FWHM/nm**
AuZRS@TB	531 ± 2	142 ± 4	553 ± 2	166 ± 4	561 ± 2	170 ± 4	564 ± 2	224 ± 4
AuZRS@TF	530 ± 2	124 ± 4	537 ± 2	106 ± 4	546 ± 2	108 ± 4	557 ± 2	104 ± 4
AuZRS@TP	517 ± 2	128 ± 4	522 ± 2	100 ± 4	529 ± 2	108 ± 4	535 ± 2	102 ± 4

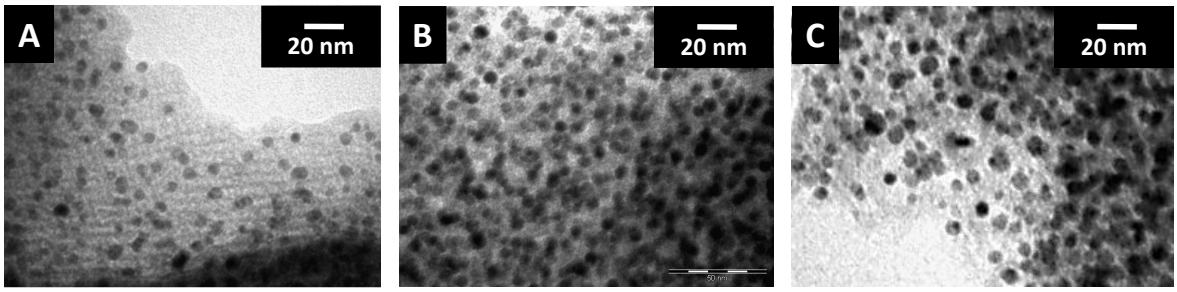

Figure S1. TEM images of **(A)** Au10RS@TB, **(B)** Au10RS@TF, and **(C)** Au10RS@TP samples.

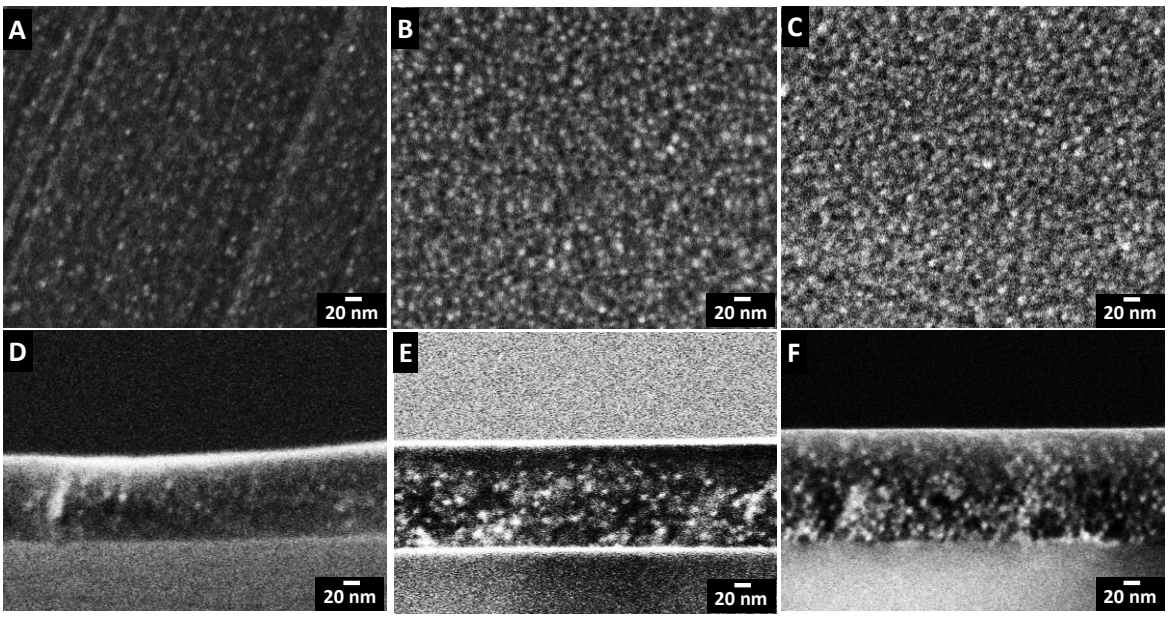

Figure S2. SEM images of **(A)** Au20RS@TB, **(B)** Au20RS@TF, and **(C)** Au20RS@TP. SEM side-view images of **(D)** Au20RS@TB, **(E)** Au20RS@TF, and **(F)** Au20RS@TP.

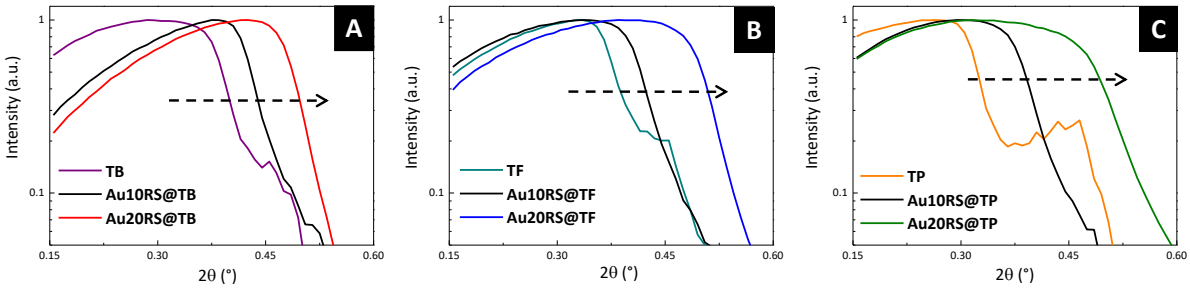

Figure S3. XRR pattern measured at RH<5% of *AuZRS@TX* samples (Z= 0, 10 and 20) for (**A**) TB, (**B**) TF and (**C**) TP.

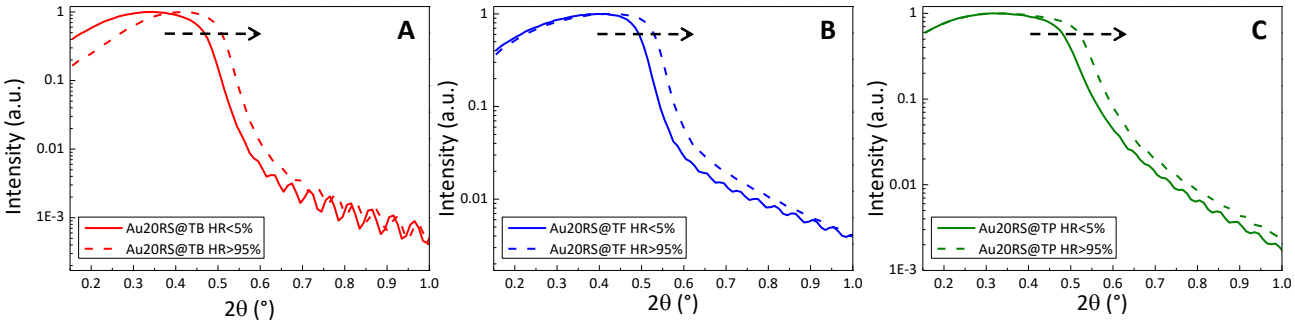

Figure S4. XRR pattern of *Au20RS@TX* samples measured at RH<5% and at RH>95% for (**A**) TB, (**B**) TF and (**C**) TP.

Changes in critical angle (RH<5% *vs* RH>95%) shows that systems are still accessible to water after NPs synthesis.

Table S3. Calculated *F (Au)* for *AuZRS@TX* samples.

	$F_v(Au)$		$F(Au)$	
	Z = 10	**Z = 20**	**Z = 10**	**Z = 20**
AuZRS@TB	0.03 ± 0.02	0.07 ± 0.02	0.05 ± 0.02	0.13 ± 0.02
AuZRS@TF	0.03 ± 0.02	0.09 ± 0.02	0.05 ± 0.02	0.17 ± 0.02
AuZRS@TP	0.04 ± 0.02	0.11 ± 0.02	0.06 ± 0.02	0.17 ± 0.02

Table S4. Au:Ti atomic ratio for *AuZRS@TX* samples, obtained by EDS.

	Au : Ti	
	Z = 10	**Z = 20**
AuZRS@TB	0.22± 0.01	0.50 ± 0.01
AuZRS@TF	0.25± 0.01	0.62± 0.02
AuZRS@TP	0.38± 0.04	0.88± 0.07

3. Overgrowth of Au NPs placed below MTTFs

Table S5. Porosity (P) and thickness of T*X* films, obtained by XRR measurements. Refractive index obtained by ellipsometry. Samples were prepared by spin-coating onto unmodified glass slides.

System	P (%)	Thickness (nm)	Refractive index
TB	48 ± 2	205 ± 5	1.65
TF	52 ± 2	170 ± 5	1.60
TP	62 ± 2	185 ± 5	1.47

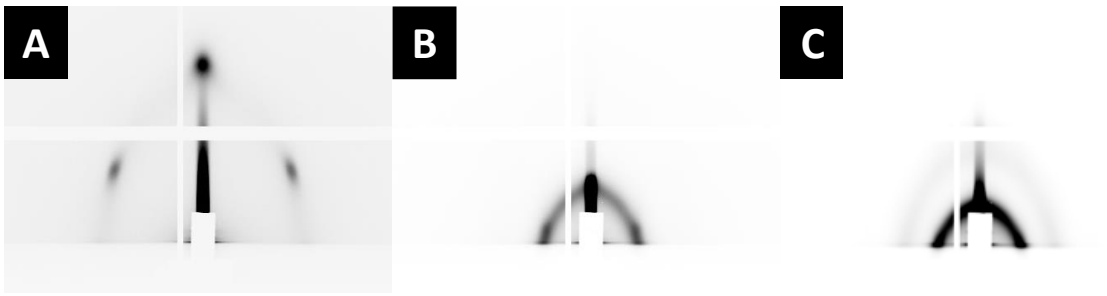

Figure S5. GISAXS patterns for **(A)** Au66/TB, **(B)** Au66/TF, and **(C)** Au66/TP systems.

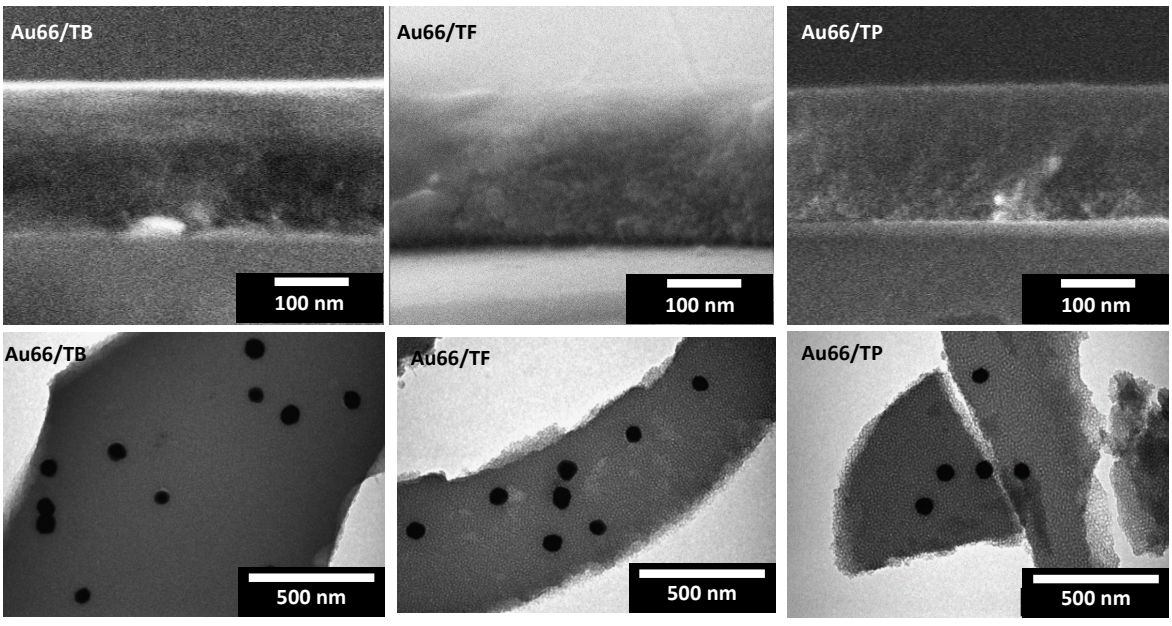

Figure S6. SEM side view (*top row*) and TEM (*bottom row*) images for *Au66/TX* samples.

Table S6. Plasmonic band maximum for *Au66/TX* samples.

	λ_{max}/nm
Au66/air	518 ± 2
Au66/TB	603 ± 2
Au66/TF	570 ± 2
Au66/TP	554 ± 2

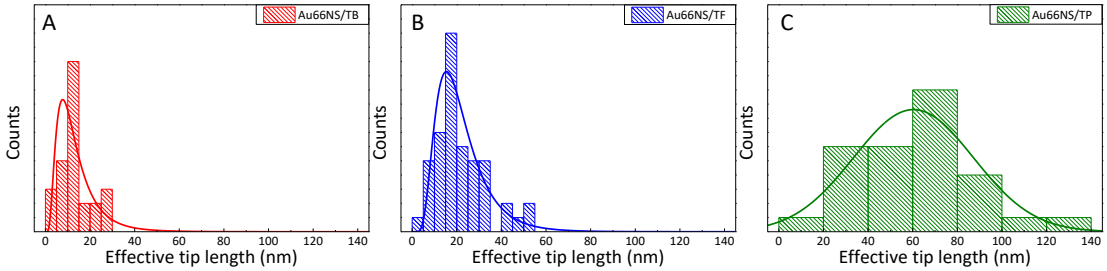

Figure S7. Effective tip length of anisotropic NPs in **(A)** Au66NS/TB, **(B)** Au66NS/TF, and **(C)** Au66NS/TP samples.

4. SERS sensing capabilities

AuZRS@TX systems

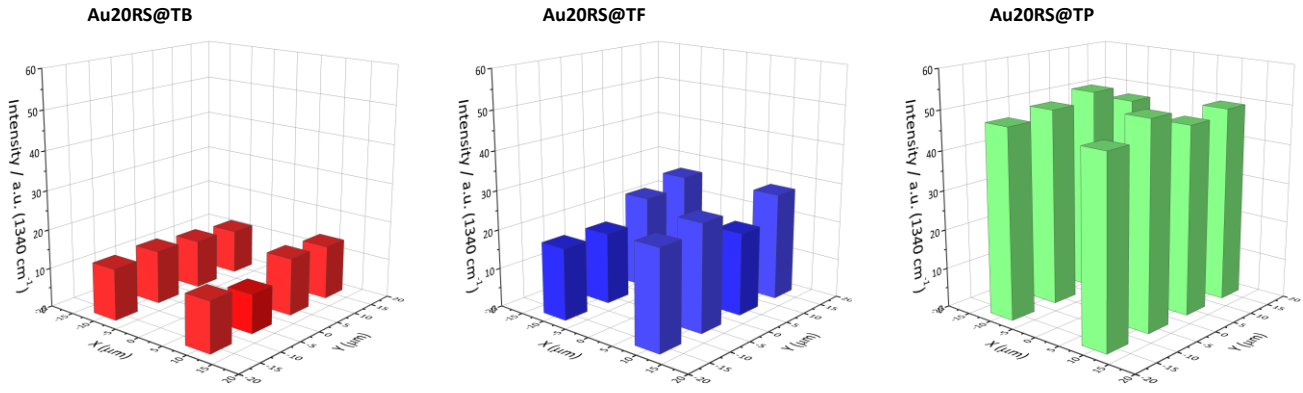

Figure S8. SERS intensity of the 1340cm^{-1} band of pNTP (acquisition time: 10 s) as a function of the interrogated spot for the different mesoporous thin films, as indicated in the labels.

High spot-to-spot reproducibility is observed.

Au66/TX systems

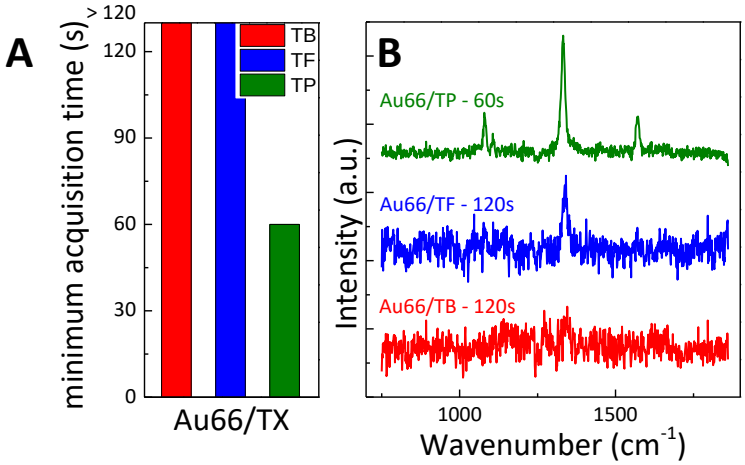

Figure S9. **(A)** Minimum acquisition time required for S > 3N for *Au66/TX* samples. **(B)** SERS spectra of pNTP: 120 s acquisition time for Au66/TB and Au66/TF, and 60 s acquisition time for Au66/TP. Each spectrum is the average of 4 spectra taken at 4 different points.

For Au66/TB signal was observed in 13% of the tested spots using 120 s, while signal was observed in 50% of the tested spots for Au66/TF. For Au66/TP signal was observed in 90% of the tested spots using 60 s.

References

1. C. Boissiere, D. Grosso, S. Lepoutre, L. Nicole, A. B. Bruneau and C. Sanchez, *Langmuir*, 2005, **21**, 12362-12371.
2. A. R. Forouhi and I. I. Bloomer, *Physical review. B, Condensed matter*, 1986, **34**, 7018-7026.